Chapter 7
Protection of Six-Phase Transmission Line Using Demeyer Wavelet Transform

Gaurav Kapoor

1 Introduction

An increase in the inevitability of electrical power has been perceived by the people of the modern generation. The electrical power transfer potentiality of the currently operating power transmission systems ought to be augmented in order to assist the significant increase in the necessity of electrical energy.

Thus, accurate recognition of the faults in the SPTL turns out to be very decisive for mitigating the loss of gain and providing fast renovates.

Numerous newly reported research works addressed the issue of FD and FC in TL's. The discussion of few researches is shown in brief here in this section. In [1], FSM-based technique has been used for TL protection. In [2, 4, 7], WT and MM have been applied for the protection of SPTL. VMD has been employed for disturbance recognition in power system [3]. POVMD and WPNRVFLN have been used for FD and FPR in SCDCTL [5]. DM and MM have been used for high impedance fault recognition in TL [6]. Alienation-based technique has been proposed for TTTL protection [8]. In [9], the theory of TW has been reported and the combination of VMD and TEO has been applied for HVDC TL protection. VMD and HT have been used for micro-grid protection [10].

In this work, the demeyer wavelet transform (DMWT) has been used for the protection of six-phase transmission line (SPTL). No such type of work has been reported yet to the best of the knowledge of author. The results exemplify that the DMWT efficiently recognizes and categorizes the faults and the consistency of the DMWT is not affected by variation in the fault factors of SPTL.

G. Kapoor (✉)
Modi Institute of Technology, Kota, India
e-mail: gaurav.kapoor019@gmail.com

M. Shorif Uddin et al. (eds.), *Intelligent Energy Management Technologies*,
Algorithms for Intelligent Systems,
https://doi.org/10.1007/978-981-15-8820-4_7

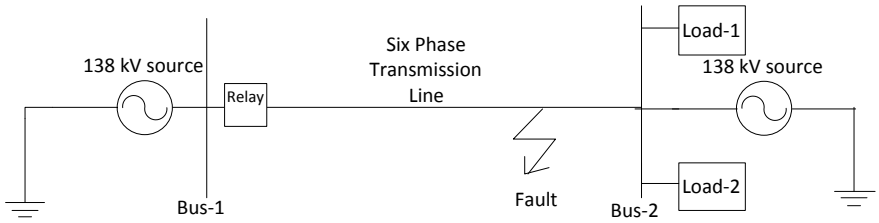

Fig. 1 The schematic of SPTL

This paper is structured as follows: The specifications of SPTL are presented in Sect. 2. The flow-diagram for DMWT is presented in Sect. 3. Section 4 is dedicated to the discussion of results. Section 5 concludes the paper.

2 The Specifications of SPTL

Figure 1 shows the schematic of SPTL. The schematic consists of 138 kV, 60 Hz SPTL of 68 km, connected to a 138 kV voltage source at one end and loads at the other end. The SPTL is divided into two parts of length 34 km each. The CT's and relay are connected at bus-1 to protect the full length of SPTL.

3 The Flow Chart of DMWT

Figure 2 illustrates the process for the DMWT. The steps are shown beneath.

Step 1 Simulate the SPTL for creating faults and produce the post-fault currents.
Step 2 Use DMWT to examine the post-fault currents for characteristics retrieval and determine the range of DMWT output.
Step 3 The phase will be proclaimed as the faulted phase if its DMWT output has a larger amplitude as compared to the healthy phase in a faulty situation.

4 Performance Assessment

The simulations have been performed for the near-in relay faults, far-end relay faults, converting faults, inter-circuit faults, and multi-position faults with the objective of verifying the feasibility of the DMWT. In the separate subcategories, the outcomes of the work are investigated.

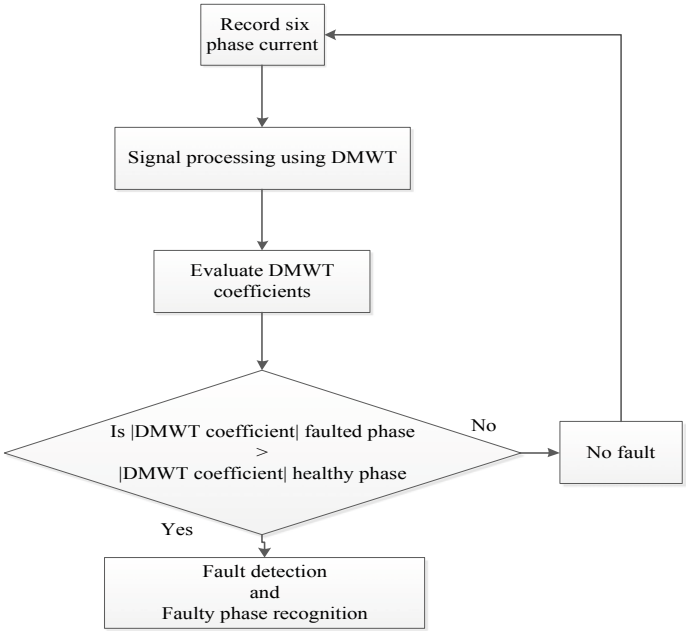

Fig. 2 Flow diagram showing DMWT process

4.1 The Efficacy of DMWT for Healthy Condition

Figure 3 shows the SPTL currents and voltages for no-fault. The DMWT outputs for no-fault are shown in Fig. 4. Table 1 reports the results of DMWT for healthy situation.

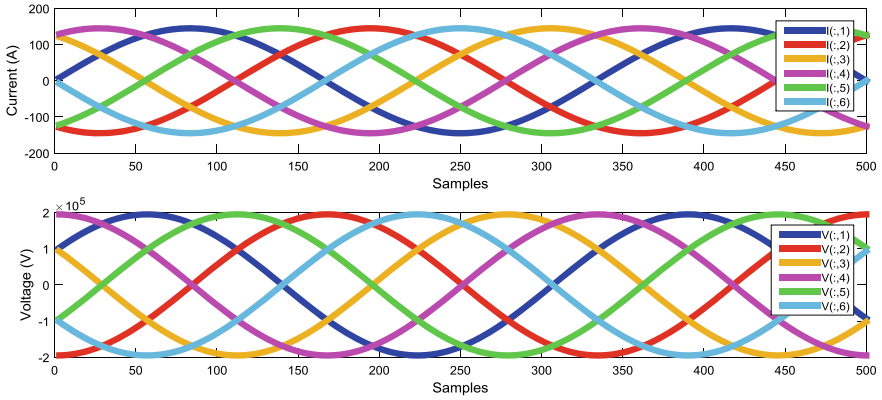

Fig. 3 Six-phase current and voltage waveforms for no-fault

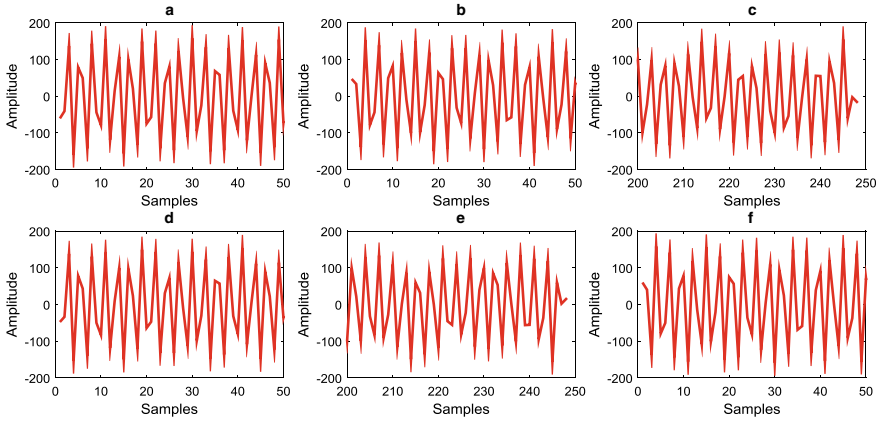

Fig. 4 DMWT outputs of six-phase currents for no-fault

Table 1 Results of DMWT for no-fault

DMWT output					
Phase-A	Phase-B	Phase-C	Phase-D	Phase-E	Phase-F
175.9988	152.7358	155.3587	154.5936	133.9446	188.1193

4.2 The Efficacy of DMWT for Near-in Relay Faults

The efficiency of the DMWT is investigated for the near-in relay faults on the SPTL. Figure 5 exemplifies the SPTL currents for ABDFG near-in relay fault at 5 km at 0.0535 s among $R_F = 2\ \Omega$ and $R_G = 4\ \Omega$. Figure 6 illustrates the DMWT output for ABDFG fault. The fault factors for the fault cases are: T = 0.0535 s, $R_F = 2\ \Omega$, and

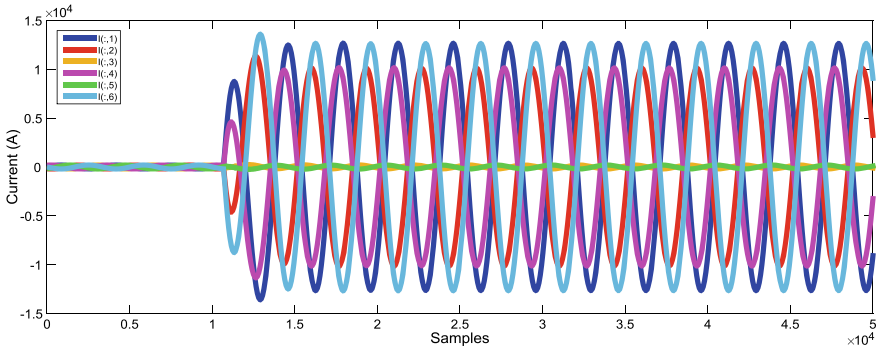

Fig. 5 ABDFG near-in relay fault at 5 km at 0.0535 s among $R_F = 2\ \Omega$ and $R_G = 4\ \Omega$

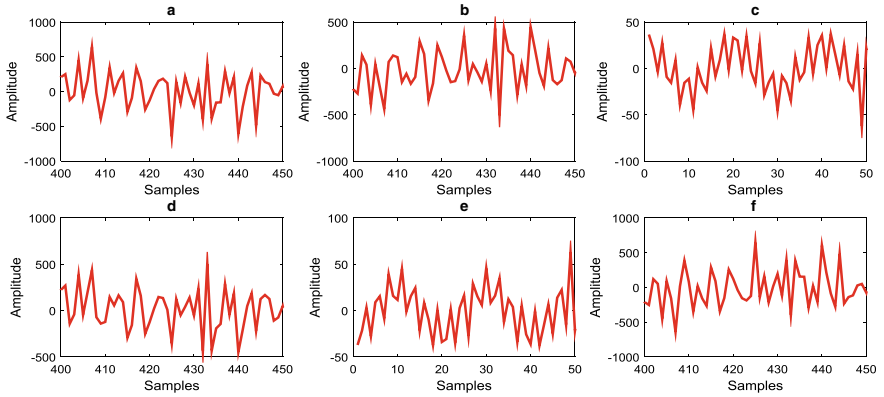

Fig. 6 DMWT output for ABDFG near-in relay fault at 5 km at 0.0535 s

Table 2 Results of DMWT for near-in relay faults

Fault type	DMWT output					
	Phase-A	Phase-B	Phase-C	Phase-D	Phase-E	Phase-F
ABDFG (5 km)	975.5428	1.5645×10^3	82.1565	905.7343	62.6620	1.4003×10^3
ABCG (6 km)	1.1302×10^3	1.0896×10^3	1.2082×10^3	86.5100	44.6221	50.1690
BCEFG (7 km)	208.6318	1.1057×10^3	1.0163×10^3	151.0041	1.3309×10^3	1.0599×10^3
ABCDEG (8 km)	1.4257×10^3	1.1870×10^3	1.1547×10^3	1.1865×10^3	993.3149	208.7100
DEFG (9 km)	53.2673	46.4882	60.4460	1.9163×10^3	1.8024×10^3	1.1828×10^3

$R_G = 4\ \Omega$. Table 2 details the results of the DMWT for near-in relay faults. It is seen from Table 2 that the DMWT precisely detects the near-in relay faults.

4.3 The Efficacy of DMWT for Far-End Relay Faults

The DMWT has been explored for the far-end relay faults. Figure 7 illustrates the SPTL currents for ABCEFG far-end relay fault at 63 km at 0.1 s among $R_F = 1.15\ \Omega$ and $R_G = 2.15\ \Omega$. Figure 8 shows the DMWT output for ABCEFG fault. Table 3 reports the results for far-end relay faults. It is inspected from Table 3 that the effectiveness of the DMWT remains unaffected for the far-end relay faults.

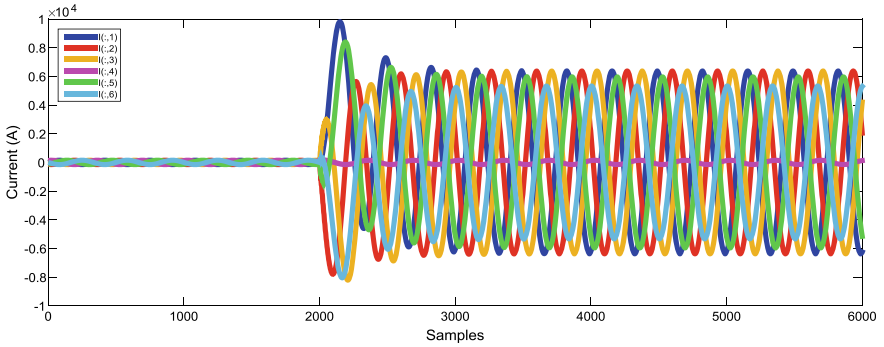

Fig. 7 ABCEFG far-end fault at 63 km at 0.1 s among $R_F = 1.15\ \Omega$ and $R_G = 2.15\ \Omega$

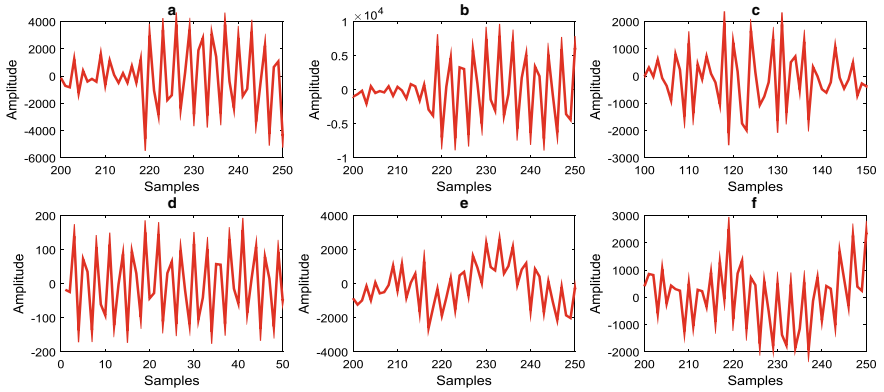

Fig. 8 DMWT output for ABCEFG far-end relay fault at 63 km at 0.1 s

Table 3 Results of DMWT for far-end relay faults

Fault type	DMWT output					
	Phase-A	Phase-B	Phase-C	Phase-D	Phase-E	Phase-F
ABCEFG (63 km)	3.8060×10^3	7.9079×10^3	4.0745×10^3	158.1244	3.4767×10^3	2.5117×10^3
ABCG (64 km)	4.8194×10^3	8.5085×10^3	4.3048×10^3	165.9761	157.4620	197.3903
DEFG (65 km)	142.1903	137.1558	124.3455	5.1810×10^3	2.7625×10^3	4.8779×10^3
ABDEG (66 km)	5.8668×10^3	6.2243×10^3	166.0415	5.8480×10^3	4.5843×10^3	153.9397
ABCDG (67 km)	3.0659×10^3	6.4599×10^3	3.7578×10^3	3.1028×10^3	197.5127	211.9889

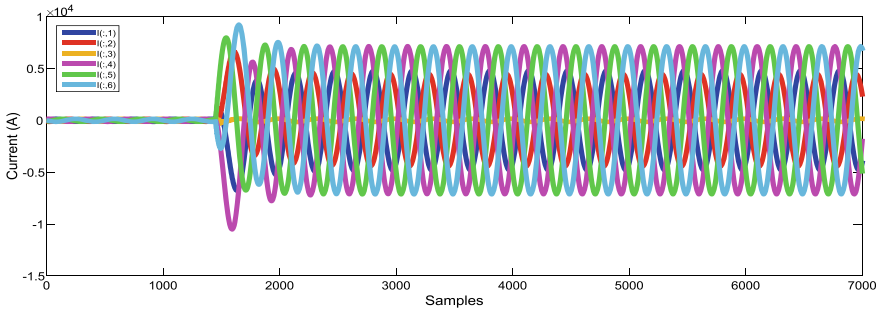

Fig. 9 SPTL currents for multi-position ABG fault at 42 km and DEFG fault at 26 km

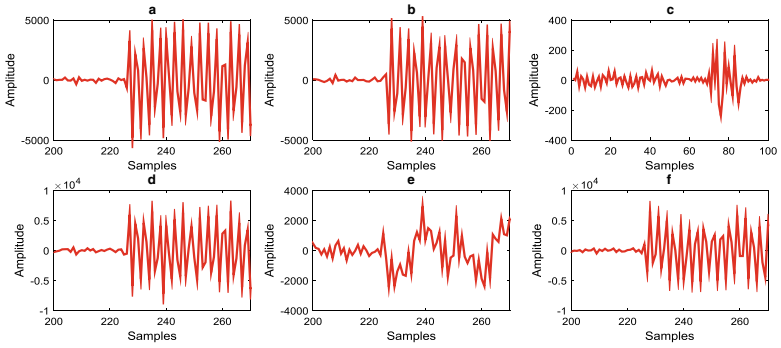

Fig. 10 DMWT output for multi-position ABG fault and DEFG fault

4.4 The Efficacy of DMWT for Multi-position Faults

The DMWT is tested for different cases of multi-position faults. Figure 9 depicts the currents when the SPTL is simulated for the multi-position ABG fault at 42 km and DEFG fault at 26 km at 0.0725 s among $R_F = 1.5\ \Omega$ and $R_G = 1.25\ \Omega$. Figure 10 shows the DMWT output for ABG and DEFG multi-position fault. Table 4 presents the results for different position-position faults.

4.5 The Efficacy of DMWT for Inter-circuit Faults

The DMWT is tested for different cases of inter-circuit faults. Figure 11 depicts the currents when the SPTL is simulated for the inter-circuit ABCG and FG fault at 30 km at 0.1325 s among $R_F = 2.75\ \Omega$ and $R_G = 1.85\ \Omega$. Figure 12 depicts the DMWT output for ABCG and FG inter-circuit fault. Table 5 reports the results for

Table 4 Results of DMWT for multi-position faults

FT-1 (km)	FT-2 (km)	DMWT output					
		Phase-A	Phase-B	Phase-C	Phase-D	Phase-E	Phase-F
ABG (42)	DFFG (26)	4.1866 × 10^3	4.4410 × 10^3	203.0695	6.5372 × 10^3	2.9300 × 10^3	6.4875 × 10^3
CG (20)	DFG (48)	248.1627	247.6852	1.4210 × 10^3	2.4488 × 10^3	179.0262	2.7339 × 10^3
DEFG (35)	BG (33)	93.2050	2.7384 × 10^3	114.9325	4.1065 × 10^3	2.7835 × 10^3	4.5857 × 10^3
ACG (44)	EFG (24)	2.4514 × 10^3	111.0308	2.0142 × 10^3	132.6308	2.8471 × 10^3	4.2729 × 10^3
DG (38)	ABCG (30)	4.8020 × 10^3	6.5308 × 10^3	2.4552 × 10^3	2.6415 × 10^3	97.7596	163.331

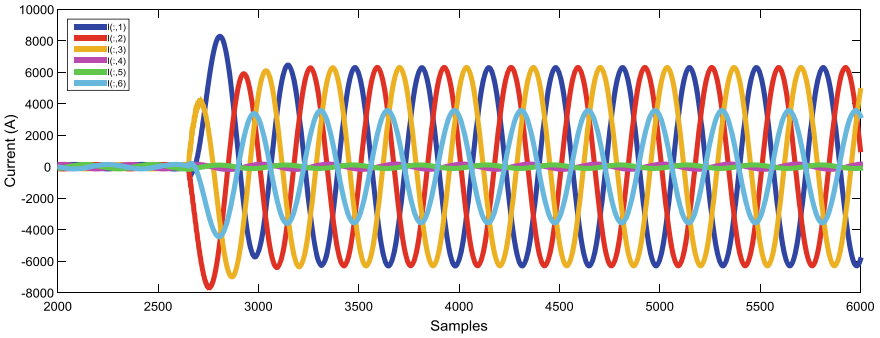

Fig. 11 SPTL currents for ABCG and FG inter-circuit fault at 30 km at 0.1325 s

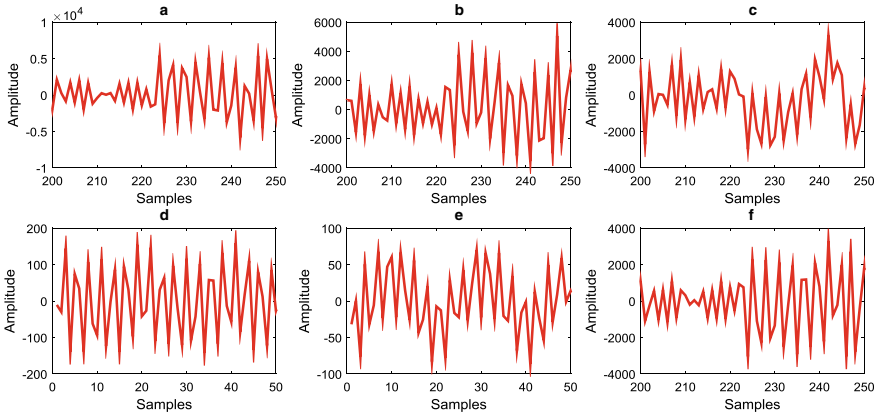

Fig. 12 DMWT output for ABCG and FG inter-circuit fault at 30 km at 0.1325 s

Table 5 Results of DMWT for inter-circuit faults

Fault-1	Fault-2	DMWT output					
		Phase-A	Phase-B	Phase-C	Phase-D	Phase-E	Phase-F
ABCG	FG	5.4287×10^3	5.0592×10^3	3.2656×10^3	159.5320	95.4246	3.3819×10^3
BG	DG	264.7818	4.0431×10^3	260.5588	3.2120×10^3	244.3075	245.0540
ACG	DEG	3.7037×10^3	176.3243	2.6696×10^3	4.8352×10^3	3.5412×10^3	131.1642
ABG	EFG	5.7039×10^3	5.8627×10^3	195.1929	201.4383	2.6028×10^3	4.5607×10^3
CG	DEFG	271.4223	202.1157	3.9056×10^3	1.0169×10^3	8.9809×10^3	4.5267×10^3

the inter-circuit faults. It is examined from Table 5 that the DMWT performs well for the recognition of inter-circuit faults.

4.6 The Efficacy of DMWT for Converting Faults

The DMWT has been investigated for the converting faults. Figure 13 exemplifies the currents of the SPTL when initially the ABG fault at 35 km at 0.05 s is converted into the DEFG fault at 35 km at 0.15 s among $R_F = 2.50\ \Omega$ and $R_G = 1.50\ \Omega$. Figure 14 exemplifies the DMWT output for the same fault case. The fault factors preferred for the additional fault cases are: $F_L = 35$ km, $R_F = 2.50\ \Omega$ and $R_G = 1.50\ \Omega$. Table 6 reports the results for different converting faults.

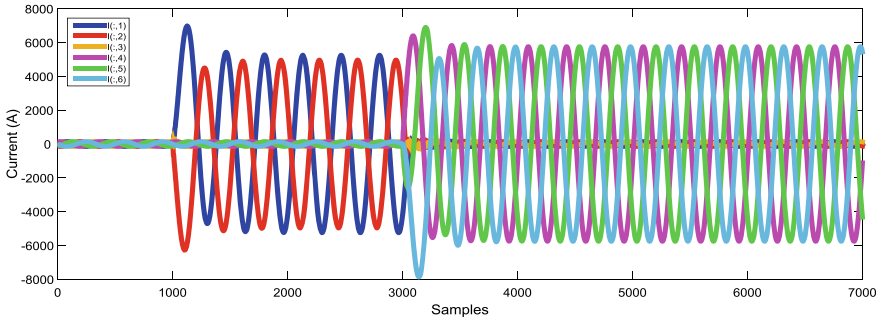

Fig. 13 SPTL current when ABG fault at 0.05 s is converted into DEFG fault at 0.15 s at 35 km among $R_F = 2.50\ \Omega$ and $R_G = 1.50\ \Omega$

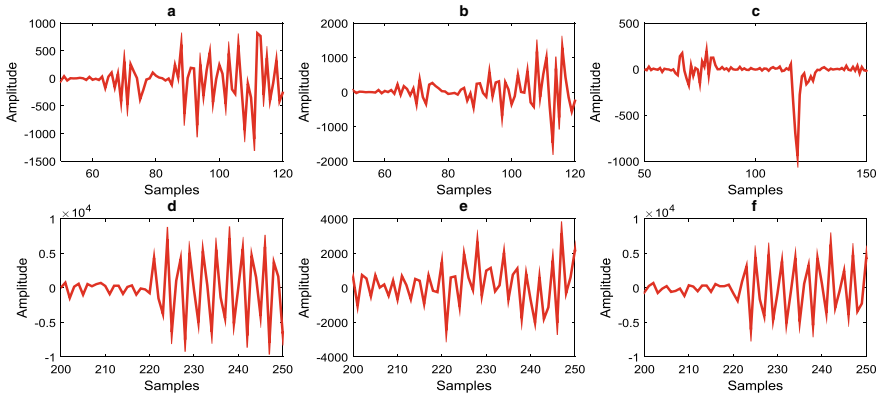

Fig. 14 DMWT output when ABG fault is converted into DEFG fault

Table 6 Results of DMWT for converting faults

Fault type	Converted fault	DMWT output					
		Phase-A	Phase-B	Phase-C	Phase-D	Phase-E	Phase-F
ABG (0.05)	DEFG (0.15)	816.6582	1.2847×10^3	196.2113	7.2091×10^3	3.1614×10^3	6.2976×10^3
DG (0.1)	DEFG (0.2)	159.9643	136.8911	198.3681	5.6853×10^3	1.7459×10^3	4.2094×10^3
ABCG (0.07)	EG (0.16)	1.5407×10^3	2.1744×10^3	1.6289×10^3	197.2483	1.3585×10^3	173.1067
ACG (0.05)	DEG (0.2)	2.0178×10^3	171.0564	1.1652×10^3	3.2852×10^3	2.0547×10^3	110.2217
EFG (0.1)	ABG (0.15)	5.8620×10^3	6.6895×10^3	208.7799	645.9092	1.4708×10^3	912.3268

5 Conclusion

The demeyer wavelet transform (DMWT) is seemed to be very efficient under varied fault categories for the SPTL. The DMWT output of fault currents of the SPTL is assessed. The fault factors of the SPTL are varied and it is discovered that the variation in fault factors do not influence the fidelity of the DMWT. The outcomes substantiate that the DMWT has the competence to protect the SPTL beside different fault categories.

References

1. Yadav A, Swetapadma A (2016) A finite-state machine based approach for fault detection and classification in transmission lines. Elect Power Component Syst (Taylor and Francis) 44(1):43–59
2. Kapoor G (2018) Six phase transmission line boundary protection using wavelet transform. In: Proceedings of the 8th IEEE India international conference on power electronics (IICPE), Jaipur, India (2018)
3. Jena MK, Samantaray SR, Panigrahi BK (2017) Variational mode decomposition-based power system disturbance assessment to enhance WA situational awareness and post-mortem Analysis. IET Gener Transm Distrib 11(13):3287–3298
4. Kapoor G (2018) Fault detection of phase to phase fault in series capacitor compensated six phase transmission line using wavelet transform. Jordan J Elect Eng 4(3):151–164
5. Sahani M, Dash PK (2019) Fault location estimation for series-compensated double-circuit transmission line using parameter optimized variational mode decomposition and weighted P-norm random vector functional link network. Appl Soft Comput J (Elsevier), 1–18 (2019)
6. Sekar K, Mohanty MK (2018) Data mining-based high impedance fault detection using mathematical morphology. Comput Elect Eng (Elsevier) 69:129–141
7. Kapoor G (2018) Six phase transmission line boundary protection using mathematical morphology. In: Proceedings of the IEEE international conference on computing, power and communication technologies (GUCON), pp 857–861, Greater Noida, India (2018)
8. Rathore B, Shaik AG (2018) Fault analysis using alienation technique for three-terminal transmission line. In: Proceedings of the IEEE 2nd international conference on power, energy and environment: towards smart technology (ICEPE), pp 1–6, Shillong, India (2018)
9. Wang L, Liu H, Dai LV, Liu Y (2018) Novel method for identifying fault location of mixed lines. Energies 11(1529):1–19
10. Chaitanya BK, Yadav A, Pazoki M (2019) An improved differential protection scheme for micro-grid using time frequency transform. Elect Power Energy Syste (Elsevier) 111:132–143